STRENGTH VARIABILITY OF DEEP CEMENT MIXED COLUMNS ON THE OVERALL PERFORMANCE OF COLUMN-SUPPORTED EMBANKMENTS

Manasi Wijerathna[1] and Samanthika Liyanapathirana[2]

[1]*GHD Pty Ltd, 29 Christie Street, St. Leonards, NSW, Australia, 2065, manasi.wijerathna@ghd.com*

[2]*School of Computing, Engineering and Mathematics, Western Sydney University, Penrith, NSW, Australia, 2751, s.liyanapathirana@westernsydney.edu.au*

ABSTRACT

Deep Cement Mixed (DCM) column improved ground is known to have large strength variability across the material domain. However, the effect of strength variability on the performance of embankments supported by DCM columns is not well studied due to scarcity of numerical modelling facilities to incorporate spatial variability of material properties directly into a finite element analysis and lack of comprehensive field monitoring data. This paper investigates the effect of spatial variability on the performance of an embankment with attached DCM column walls beneath the side slopes. The analysis was carried out using numerical models developed using ABAQUS finite element program incorporating the spatial variability of DCM columns. The strength field in the material domain was randomly generated, from a lognormal distribution, using a computer program written in MATLAB. The sensitivity of embankment deformations to spatial correlation length, coefficient of variation (COV) and partial factor of safety (PFOS) was investigated by analysing a series of models. The reliability of the embankment in each analysis case was assessed using 1500 Monte Carlo realizations. Results demonstrate that the spatial correlation length of strength properties has a great influence on the reliability-based performance of the embankment. Larger spatial correlation lengths resulted higher upper bound in the lateral deformation data of the embankment. COV also affected the upper and lower bounds of the lateral deformation data. The PFOS significantly affected the skewness of the deformation distribution, however PFOS does not affect the upper and lower bounds of the distribution.

Key words: Spatial variability, Reliability based performance, Deep cement mixing, Finite element modelling, Monte Carlo method

1. INTRODUCTION

Deep cement mixing is a well-developed ground improvement technology that is in practice in many regions around the world. However, achieving uniform material properties in Deep Cement Mixed (DCM) soils is highly unrealistic due to several influence factors such as; non uniform mixing, natural variability in the ground and non uniform curing conditions. As a result, DCM soils show a large variability of properties over the material space. The coefficient of variation (COV) is a measure of the degree of strength variability in a material, which is derived as the standard deviation normalized by the mean strength. According to the literature, COV of DCM soil strength normally varies from 0.3 to 0.8 (Filz and Navin 2010; Kasama et al. 2012; Larsson et al. 2005b). While the strength properties of DCM soil are spatially variable, the strength field is also spatially correlated (Honjo 1982). The reported horizontal and vertical correlation lengths vary from 0 to 12 m (Al-Naqshabandy et al. (2012a), Kasama et al. (2012), Liu et al. (2015)). In comparison to the dimensions of a typical embankment, these correlation lengths are small. These correlation lengths suggest that the strength properties of DCM soil can gradually vary within a single project resulting localized zones of low and high strengths. Therefore, design of DCM column-supported embankments assuming uniform DCM soil strength properties is not a realistic representation of the actual situation.

Many reliability studies considering spatial variability in natural soils are available in the literature (e.g. Jiang and Huang (2016), Kasama and Zen (2011), Liu et al. (2017a)). However, the studies specific to spatial variability in DCM soils are limited (Kasama et al. 2012; Liu et al. 2015; Namikawa 2016; Namikawa and Koseki 2013; Zhang et al. 2017). In some cases, the reliability based performance was investigated considering natural and cement mixed soils as a composite system (Al-Naqshabandy and Larsson 2013; Al-Naqshabandy et al. 2012b; Huang et al. 2015; Navin 2005; Navin and Filz 2006). All these studies highlighted the importance of spatial correlation length in establishing the strength profile of DCM soil in reliability studies.

In this study, the performance of an embankment with side slopes supported on DCM wall panels was evaluated considering the spatial variability of strength properties, using a reliability based approach. The analysis was carried out using two-dimensional plane-strain finite element models developed using the ABAQUS/Standard

(2014) finite element program. Material properties for different cases were randomly generated from a lognormal distribution with a specific mean strength and a COV using a computer program written in MATLAB. The ABAQUS/Standard (2014) finite element analysis was executed for each case within this MATLAB program. The finite element analyses were based on a coupled analysis where pore water pressure generation and dissipation were included. Reliability was evaluated using the Monte Carlo method. A series of reliability analyses were conducted assuming finite spatial correlation distances. The embankment performance was investigated for different mean strengths, coefficients of variation and spatial correlation lengths to identify the sensitivity of spatial variability on the reliability of the embankment performance.

2. NUMERICAL MODEL

The analysis was carried out using two-dimensional plane-strain numerical models developed using the ABAQUS/Standard (2014) finite element program. In this study, DCM panels beneath the embankment slopes were converted to a plane-strain model based on the equivalent properties approach. Accordingly, the width and height of the DCM panel were not changed and the equivalent properties for DCM panels (E_{eq}, c'_{eq} and φ'_{eq}) were calculated using Equations 1 to 3 (Ariyarathne et al. 2013; Chan and Poon 2012; Huang et al. 2009; Yapage et al. 2014).

$$E_{eq} = E_c a_r + E_s(1 - a_r) \tag{1}$$

$$c'_{eq} = c'_c a_r + c'_s (1 - a_r) \tag{2}$$

$$\phi'_{eq} = \tan^{-1}\left(\frac{(1 - a_r)\tan\phi'_s + n a_r \tan\phi'_c}{(1 - a_r) + n a_r}\right) \tag{3}$$

where E_{eq}, E_c and E_s are the elastic modulus of the equivalent panel, DCM panels and the surrounding soil, respectively; a_r is the area replacement ratio of DCM panel; c'_{eq}, c'_c and c'_s are the effective cohesion of the equivalent panel, DCM panels and the surrounding soil, respectively; and φ'_{eq}, φ'_c and φ'_s are the effective friction angle of the equivalent panel, DCM panels and the surrounding soil, respectively and n is the ratio of stress over DCM wall to stress over surrounding soil, known as the stress concentration ratio. The value of n was considered as 3.5 in this study, which is based on the average stress concentration ratio calculated using a three-dimensional numerical model of the embankment.

2.1. EMBANKMENT GEOMETRY AND BOUNDARY CONDITIONS

Figure **1** shows the geometry of the embankment selected for this study. The embankment has a height of 5.5 m and a width of 30 m at the crest level. The gradient of the embankment side slopes is 2:1 and the width of the embankment at the base level is 52 m. There is a 10 m thick soft clay layer immediately below the embankment fill, underlain by a 5 m thick silty sand layer and a 5 m thick stiff to hard clay layer, respectively. The soft clay layer beneath the slope of the embankment was improved with DCM panels with a width of 11 m and a height of 10 m. Normally wall panels are used underneath sloping sides to minimise the lateral deformations and to improve the stability of the embankment (Yapage et al. 2014). Each DCM wall panel consists of eighteen 0.8 m diameter attached DCM columns with 0.2 m overlap. The panels were spaced at 2 m in the longitudinal direction of the embankment. Hence, the area replacement ratio (ARR) beneath the side slopes was 35.5%. The ground-water table was at the ground surface. A geosynthetic layer was placed at 0.25 m above the ground surface.

The embankment was constructed in 5 stages. The first four fill layers have a thickness of 1 m and each layer was constructed over a period of 10 days at a uniform rate of 0.1 m/day. A 1.5 m thick fill layer was added during the fifth stage over 15 days.

The variability incorporated analysis was carried out using half of the embankment geometry assuming symmetry of the embankment, which will assist to save analysis time and computer memory during the Monte Carlo simulations. Since the DCM panel is located 15 m away from the centreline of the embankment, the influence of the strength variability of the DCM wall on the deformations at the centreline is very small. Therefore, a symmetrical boundary condition at the centreline was considered as a reasonable assumption for this problem, although it is not symmetrical with respect to material space. The vertical boundary at the far end of the embankment was set at 60 m away from the toe of the embankment and the deformations were restrained in the horizontal direction. At the bottom of the subsoil deposit (stiff to hard clay layer), movements were restricted in both vertical and horizontal directions. A zero pore water pressure boundary was set along the level

of the water table. Coupled effective stress – pore water pressure analysis was carried out, below the ground-water level. The bottom boundary and the two vertical boundaries were considered as impermeable.

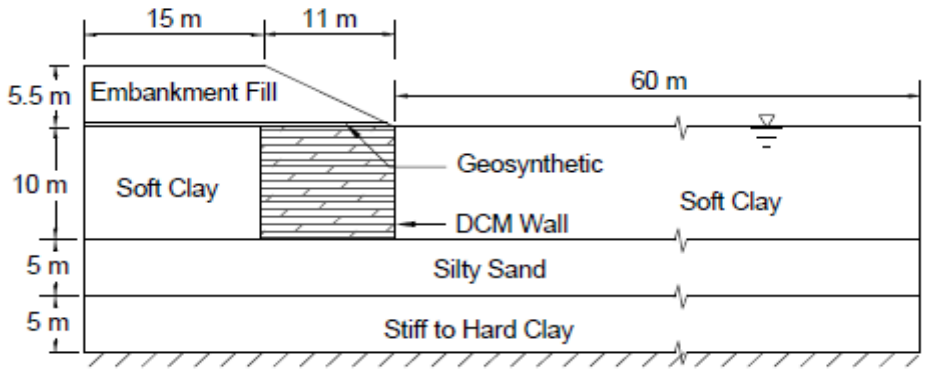

Figure 1: Geometry of the embankment and layout of DCM walls and geosynthetic reinforcement layer

2.2. FINITE ELEMENT MESH AND MATERIAL MODELS

The soil layers and DCM walls were modelled using eight-node quadrilateral elements with reduced integration and pore pressure degrees of freedom at the corner nodes (CPE8RP). Eight-node quadrilateral elements with reduced integration and without pore pressure degrees of freedom (CPE8R) were used to model the embankment fill. The three soil layers, DCM panel and the embankment fill were modelled using the Mohr-Coulomb material model. Although an extended version of Mohr-Coulomb model incorporating strain-softening behaviour has been proposed by the authors for DCM columns, in this paper Mohr-Coulomb model with elastic, perfectly plastic behaviour has been adopted to reduce the complexity of Monte-Carlo simulations. The geosynthetic layer was modelled using three-node quadratic truss elements (T2D3), which do not resist bending and compressive stresses but resists tensile stresses.

2.3. SELECTION OF MATERIAL PARAMETERS

The material properties used for DCM walls, soft clay layer, silty sand layer and stiff to hard clay layer and embankment fill are shown in Table **1**. The elastic modulus, E_c, and the effective cohesion, c'_c, of the DCM soil are considered as proportional to the unconfined compressive strength, q_u, of the DCM soil. The relationship between the elastic modulus and the unconfined compressive strength of DCM soil was assumed as $E_c = 100q_u$ (Bruce and Bruce 2003; Huang et al. 2009; Yapage and Liyanapathirana 2014). According to the literature, the cohesion of DCM soil varies within the range of $0.2q_u$ – $0.5q_u$ (Andromalos et al. 2000; Broms 1999; Euro Soil Stab 2002; Yapage et al. 2014). Therefore, the effective cohesion of DCM soil was assumed as $c'_c = 0.4q_u$. Same relationships were used to vary E_c and c'_c in proportionate to the strength of DCM soil in the probabilistic analysis. The recommended values for the drained friction angle, ϕ'_c, of DCM soil ranges from 30^0-35^0 (Broms 1999; Euro Soil Stab 2002). Since ϕ'_c varies over a small range for DCM panels, it was considered as a deterministic parameter with a value of 30^0.

Table 1: Material properties used for DCM wall, soft clay, silty sand and stiff to hard clay

Parameter	DCM Wall	Soft clay	Silty sand	Stiff to hard clay	Embankment fill
Saturated unit weight, γ_{sat} (kN/m^3)	18	18	18	16.5	19
Permeability , κ (m/s)	5×10^{-8}	5×10^{-8}	8.3×10^{-7}	5.3×10^{-7}	-
Poisson's ratio, ν	0.3	0.3	0.3	0.3	0.3
Effective cohesion , c' (kPa)	250	1	1	1	10
Elastic modulus , E (MPa)	62.5	5	15	17	20
Drained friction angle , φ'	30^0	25^0	30^0	25^0	30^0

The geosynthetic reinforcement was assumed to have an elastic modulus of 100 MPa, yield strength of 75 MPa and a Poisson's ratio of 0.3. The thickness was assumed as 1 mm. The interaction between the geosynthetic layer and the embankment fill material was modelled as a surface to surface contact with an interface friction coefficient of 0.8.

3. RELIABILITY-BASED PERFORMANCE OF THE EMBANKMENT

In this section, a probabilistic analysis was carried out considering the variability of strength properties of DCM panels to evaluate the reliability based performance of the embankment. The strength variability was introduced to the model considering spatially varying strength properties with spatial correlation, within a DCM panel. The main function of DCM panels is to resist the lateral deformations in the subsoil closer to the toe of the embankment. Therefore, the maximum lateral deformation beneath the toe of the embankment was used to monitor the performance of the embankment in the probabilistic analysis. For the current analysis, the target deformation was set as 34 mm, which is the lateral displacement beneath the toe of the embankment corresponding to a deterministic analysis with DCM panel strength of 625 kPa. A tolerance of 10% was allowed for the lateral deformation in the probabilistic analysis. Therefore, an embankment exceeding 37.5 mm lateral displacement beneath the toe of the embankment was considered as an unsatisfactory performance. The probability of unsatisfactory performance, P_u, was obtained as the ratio of frequency of unsatisfactory performance to the number of Monte Carlo realisations. 1500 Monte Carlo realisations were used in this study.

Table 2: Parameters used in the probabilistic study

DCM column properties	Range of values
Mean strength, μ_q (kPa)	625, 750, 1000, 1250
PFOS	1, 1.2, 1.5, 2
Effective cohesion, c'_c	$0.4q_u$
Friction angle, φ'	30^0
Elastic modulus, E_c	$100q_u$
COV	0.3, 0.5, 0.7
Monte Carlo iterations	1500
Spatial correlation length, θ	0, 0.5, 1, 2, 4

The compressive strength, elastic modulus and effective cohesion of DCM soil were considered as stochastic parameters in the probabilistic analysis. The c'_c and E_c were varied in proportionate to q_u as discussed in the "Selection of material parameters" section. The strength variability within the surrounding natural soil was not incorporated into this study. Many studies have shown that both lognormal and normal distributions are suitable to characterise the strength distribution within DCM soil (Honjo 1982; Kasama et al. 2012; Namikawa and Koseki 2013; Navin 2005). In this study, the compressive strength of DCM soil was assumed to have a lognormal distribution with a specific mean strength and variance instead of a normal distribution to avoid generating negative stiffness and strength properties within the material space.

According to the literature, spatial correlation lengths in DCM improved ground are different in the horizontal and vertical directions (Al-Naqshabandy et al. 2012a; Larsson et al. 2005b; Tang et al. 2001). However, data for cross correlation between horizontal and vertical spatial correlation lengths are not available. Therefore, in this analysis correlation length was assumed as equal in all directions within the plane of the panel. Table 2 shows the parameters used in the analysis.

3.1. RELIABILITY ANALYSIS

DCM panel strength values were randomly generated from a lognormal distribution with a specific mean strength and a COV using a computer program written in MATLAB. The ABAQUS finite element analysis was executed for each case within the MATLAB program.

The autocorrelation function shown in Equation 4 was used to determine the correlation coefficient of compressive strength between two nodes in the DCM panel (Honjo 1982; Namikawa and Koseki 2013).

$$\rho(d) = \exp\left(-\frac{d}{\theta}\right) \tag{4}$$

where ρ(d) is the correlation coefficient, d is the distance between two nodes and θ is the spatial correlation length.

The compressive strength at ith node, q_i, is a lognormally distributed random field with mean, μ_q, coefficient of variation, COV_q, and spatial correlation distance θ and was calculated as:

$$q_i = \exp\left(\mu_{\ln q} + \sigma_{\ln q} \cdot G_i\right) \tag{5}$$

where $\mu_{\ln q}$ and $\sigma_{\ln q}$ are calculated using Equations 6 and 7, and G_i is a random variable with a spatial correlation distance of θ, calculated using equation 8. The range of G_i was bounded between +4 and -4 to avoid extremely large or small q_i values.

$$\sigma_{\ln q} = \sqrt{\ln\left(1 + COV_q^2\right)} \tag{6}$$

$$\mu_{\ln q} = \ln \mu_q - \frac{1}{2}\sigma_{\ln q}^2 \tag{7}$$

$$G_i = CR_n \tag{8}$$

where, C is the Cholesky decomposition of the correlation coefficients matrix and R_n is a normally distributed random variable with zero mean and unit variance.

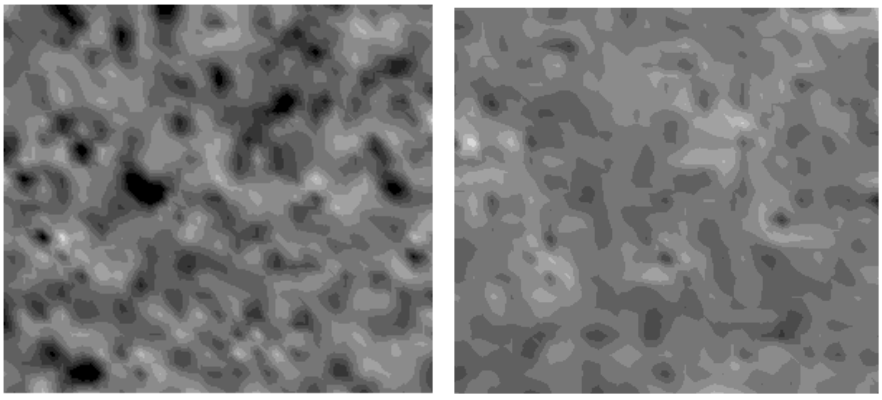

(a) (b)

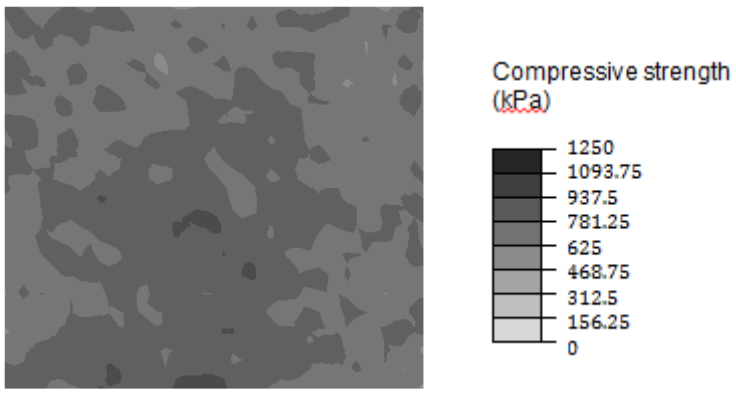

(c)

Figure 2: Typical samples of compressive strength profiles within DCM panel when spatial correlation length is (a) 0 m, (b) 1 m, (c) 4 m

This procedure was repeated for each Monte Carlo realisation to generate different strength profiles in the DCM panel. The elastic modulus and cohesion were changed across the DCM panel in proportionate to q_i as discussed in the "Selection of material parameters" section. The compressive strength profiles in the DCM panel generated in typical Monte Carlo realisations for cases with different correlation distances are shown in 2. In Figure , darker regions indicate higher strengths and lighter regions indicate lower strengths.

Figure 2 shows the performance levels of the embankment with different spatial correlation lengths for the case with mean strength of 625 kPa. P_u was less than 1/1500 for all the considered spatial correlation distances when the COV was 0.3. For the cases with COV 0.5 and 0.7, P_u was maximum when spatial correlation length was 2 m. The ratio of the spatial correlation length corresponding to the peak P_u to the width of DCM wall is 0.18. P_u reduced when correlation length is greater than 2 m. A strength profile with a small spatial correlation length indicates a highly variable strength distribution over the material space. Therefore any possible failure surface may encounter both strong elements and weak elements in equal proportions. As a result, P_u decreases towards zero, when spatial correlation length reduces below 2 m.

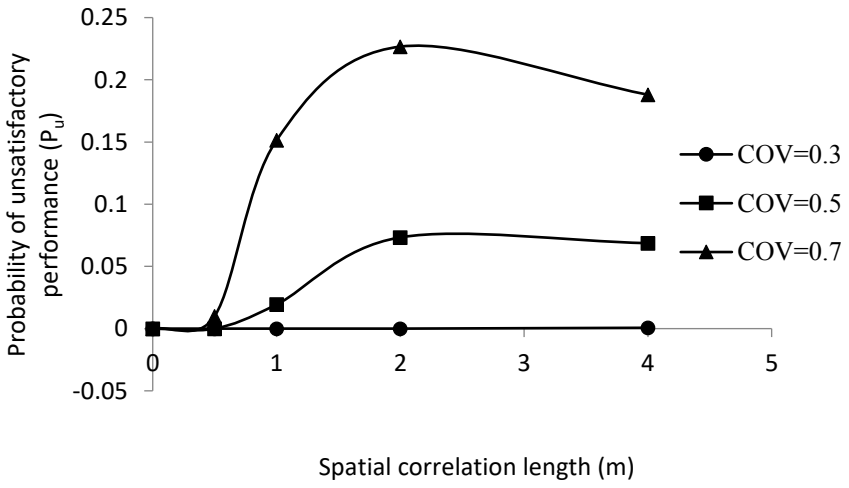

Figure 2: Reliability based performance of the embankment

3.2. OBSERVED TRENDS IN THE MONTE CARLO SIMULATION RESULTS

The maximum lateral displacement beneath the toe of the embankment is expected to vary linearly with the strength of the DCM wall panel when the panel strength is uniform over the section. Therefore, the Monte Carlo simulation that assumes uniform strength of DCM wall and lognormal distribution of strength values among the

realisations produces a set of maximum lateral deformations that fit into a lognormal distribution. However, when the DCM panel strength varies spatially, the type of distribution of the resulting lateral deformations cannot be pre-determined. An attempt was taken in this study to identify the type of distribution of the lateral deformation data generated from Monte Carlo simulations. Figure 3 shows results from three cases along with their normal and lognormal probability density functions. The deformation data generated from Monte Carlo realisations show a poor fit with normal and lognormal probability distributions. Hence, the P_u predicted using the best fit normal and lognormal distributions largely differed from the P_u values obtained from the Monte Carlo simulations (Figure 4).

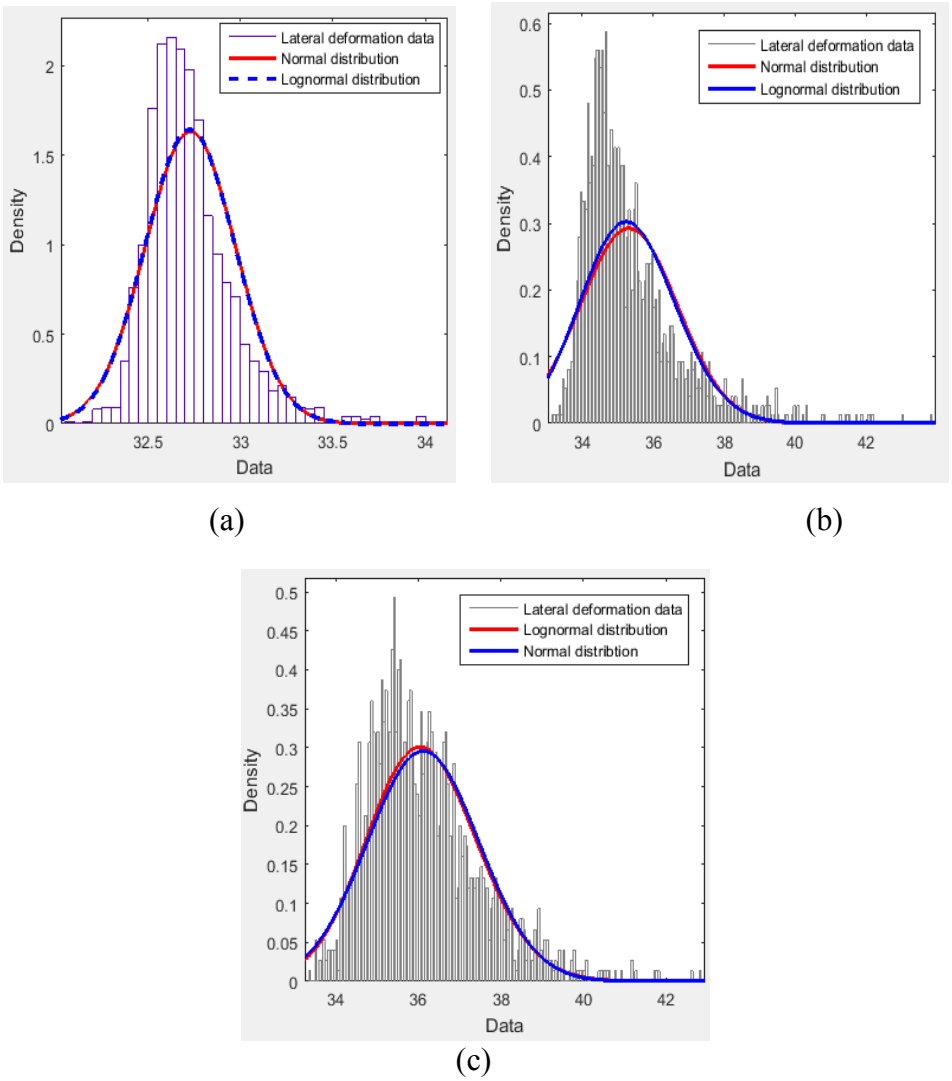

Figure 3: Best fit normal and lognormal distributions for the lateral deformation data obtained from Monte Carlo simulations (a) PFOS=2, COV= 0.3 and θ = 2 m; (b) PFOS=1, COV= 0.5 and θ = 2 m and (c) PFOS=1, COV= 0.7 and θ = 1 m

Although the Monte Carlo simulation results do not fit into a probability distribution, the deformation data showed some trend with changing characteristics of the strength field. Table 3 shows the change in lateral deformation data with increasing spatial correlation length, when PFOS=1 and COV=0.7. The lower bound of the lateral deformation data do not change more than 1 mm when spatial correlation length varied between 0 to 4 m. The upper bound of the deformation data increased gradually from 34.7 mm to 47.3 mm with increasing spatial correlation length from 0 to 4 m. As a result, the span of the deformation data distribution also increased with increasing spatial correlation length. The lateral deformation data tend to deviate more from a normal or lognormal distribution with increasing correlation length.

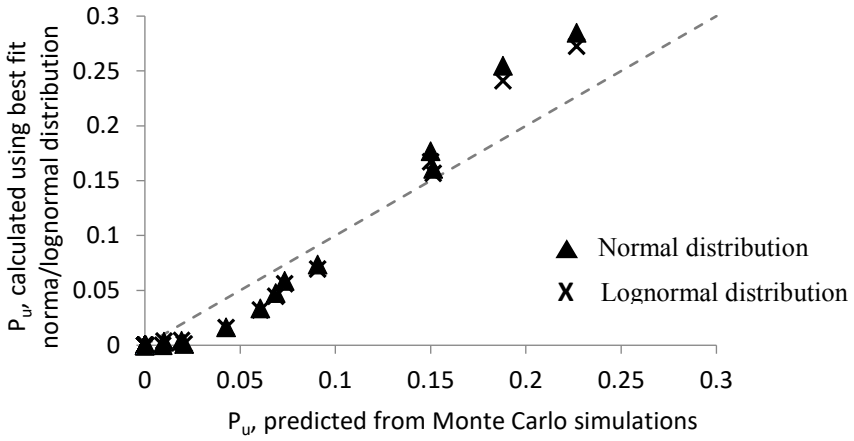

Figure 4: P_u predicted from Monte Carlo simulations Vs P_u calculated using best fit probability distributions

Table 3: Changes in the distribution of lateral deformation data when increasing spatial correlation length (PFOS=1 and COV=0.7)

Spatial correlation length, θ	0	0.5 m	1 m	2 m	4 m
Lower bound (mm)	33.696	34.039	33.388	33.172	33.294
Upper bound (mm)	34.668	39.949	42.817	46.505	47.307
Span of the distribution (mm)	0.972	5.91	9.429	13.303	14.013

As shown in Table 4, both upper and lower bounds of the lateral deformation data changed slightly with increasing PFOS. The difference in the span of data is also less than 1 mm between the four cases shown in Table 4. This indicates that PFOS does not change the upper and lower bounds of the data set. However, the skewness of the data distributions increased in the positive direction with increasing PFOS.

Table 4: Changes in the distribution of lateral deformation data when increasing PFOS (COV=0.7 and θ=2 m)

PFOS	1	1.2	1.5	2
Lower bound (mm)	33.172	32.402	31.733	31.437
Upper bound (mm)	46.505	46.408	46.028	45.644
Span of the distribution (mm)	13.303	14.001	14.295	14.207
Skewness	1.3872	1.5082	1.7105	1.9041

Changes in the lateral deformation data with increasing COV are shown in

Table **5**. The lower bound did not vary significantly with changing COV. The upper bound and the span of lateral deformation data increased with increasing COV.

Table 5: Changes in the distribution of lateral deformation data when increasing COV (PFOS=1 and θ= 2 m)

COV	0.3	0.5	0.7
Lower bound (mm)	33.491	33.166	33.172
Upper bound (mm)	37.285	43.808	46.505
Span of the distribution (mm)	3.794	10.642	13.303

4. CONCLUSIONS

This study investigates the performance of a DCM panel supported embankment beneath the slopes, using reliability based approach. The spatial variation of strength properties of DCM panels were incorporated in this analysis along with the spatial correlation characteristics. The strength field within DCM panel was varied among the different realisations of Monte Carlo simulations. The analysis was carried out for 21 analysis cases considering different combinations of spatial correlation length, coefficient of variation (COV) and partial factor of safety (PFOS). 1500 Monte Carlo realisations were carried out for each analysis case and the probability of unsatisfactory performance, P_u , was predicted. Results of this study show that a peak for P_u was observed when spatial correlation distance was 0.18 times the width of the DCM wall. P_u reaches zero with decreasing correlation length below 2 m as well as decreasing COV. The deformation data obtained from Monte Carlo simulations incorporating spatial variability of strength properties did not fit well into a normal or lognormal probability distribution. However, the lateral deformation data showed some clear response to changing spatial correlation length and COV of the input strength field. The upper bound and the span of the deformation data increased with increasing spatial correlation length and COV. The skewness of the deformation distribution shifted to left with increasing PFOS. The upper and lower boundaries of the lateral deformation data were not affected by the PFOS. Although these results cannot be directly applied to field problems, they clearly show how the variability if material properties influence the overall performance of embankments. Unsatisfactory performance changes with both COV and correlation length. If a 10% tolerance is allowed, it can be achieved with COV of 0.3, irrespective of the spatial correlation length of the DCM strength within wall panels.

5. REFERENCES

ABAQUS/Standard. (2014). *ABAQUS version 6.14 - Computer software*, Dassault Systèmes Simulia Corp., Providence, Rhode Island, USA.

Al-Naqshabandy, M.S., Bergman, N.S., and Larsson, S. (2012a). "Strength variability in lime-cement columns based on CPT data." *Ground improvement*, 165(1), 15-30.

Al-Naqshabandy, M.S., and Larsson, S. (2013). "Effect of uncertainties of improved soil shear strength on the reliability of embankments." *Journal of Geotechnical and Geoenvironmental Engineering*, 139(4), 619-632.

Al-Naqshabandy, S., Bergman, N., and Larsson, S. (2012b). "Effect of Spatial Variability of the Strength Properties in Lime-Cement Columns on Embankment Stability." *Proceedings of the Fourth International Conference on Grouting and Deep Mixing*, New Orleans, Louisiana, United States, 231-242,February 15-18, 2012.

Andromalos, K.B., Hegazy, Y.A., and Jasperse, B.H. (2000). "Stabilization of soft soils by soil mixing." *Proceedings of the Soft Ground Technology Conference, United Engineering Foundation and ASCE Geo-Institute, Noordwijkerout, Netherlands*,May 28 – June 2.

Ariyarathne, P., Liyanapathirana, D.S., and Leo, C.J. (2013). "Comparison of different two-dimensional idealizations for a geosynthetic-reinforced pile-supported embankment." *International Journal of Geomechanics*, 13(6), 754-768.

Broms, B.B. (1999). "Keynote lecture: Design of lime, lime/cement and cement columns." *International Conference on Dry Mix Methods: Dry Mix Methods for Deep Soil Stabilization*, Balkema, Rotterdam, 125-153.

Bruce, D.A., and Bruce, M.E.C. (2003). "The practitioner's guide to deep mixing. ." *Grouting and Ground Treatment, Geotechnical Special Publication No. 120*, 474-488.

Chan, K., and Poon, B.O.S.C.O. (2012). "Designing stone columns using 2D FEA with equivalent strips." *Proc., Int. Conf. on Ground Improvement and Ground Control*, 2, 609-620.

Cho, S.E. (2007). "Effects of spatial variability of soil properties on slope stability." *Engineering Geology*, 92(3), 97-109.

Euro Soil Stab. (2002). "Development of design and construction methods to stabilize soft organic soils: design guide soft soil stabilization"*CT97-0351, Project No. BE 96-3177*. Industrial and materials technologies programme (Brite-EuRam III), European Commission.

Fenton, G.A., and Griffiths, D.V. (2008). *Risk assessment in geotechnical engineering*, John Wiley and Sons.

Filz, G.M., and Navin, M.P. (2010). "A practical method to account for strength variability of deep-mixed ground." *GeoFlorida 2010: Advances in Analysis, Modeling & Design, Geotechnical special publication No. 199*, 2426-2433.

Honjo, Y. (1982). "A probabilistic approach to evaluate shear strength of heterogeneous stabilized ground by deep mixing method." *Soils and Foundation*, 22(1), 23-38.

Huang, J., Griffiths, D.V., and Fenton, G.A. (2010). "System reliability of slopes by RFEM." *Soils and Foundations*, 50(3), 343-353.

Huang, J., Han, J., and Oztoprak, S. (2009). "Coupled mechanical and hydraulic modeling of geosynthetic-reinforced column-supported embankments." *Journal of Geotechnical and Geoenvironmental Engineering*, 135(8), 1011-1021.

Huang, J., Kelly, R., and Sloan, S.W. (2015). "Stochastic assessment for the behaviour of systems of dry soil mix columns." *Computers and Geotechnics*, 66, 75-84.

Jiang, S.-H., and Huang, J.-S. (2016). "Efficient slope reliability analysis at low-probability levels in spatially variable soils." *Computers and Geotechnics*, 75, 18-27.

Kasama, K., Whittle, A.J., and Zen, K. (2012). "Effect of spatial variability on the bearing capacity of cement-treated ground." *Soils and Foundations*, 52(4), 600-619.

Kasama, K., and Zen, K. (2011). "Effects of spatial variability of soil property on slope stability." *Vulnerability, Uncertainty, and Risk Analysis, Modeling and Management, 2011 conference*, Reston, VA, USA, 691–698.

Larsson, S., Stille, H., and Olsson, L. (2005). "On horizontal variability in lime-cement columns in deep mixing." *Géotechnique*, 55(1), 33-44.

Liu, L.-L., Cheng, Y.-M., and Zhang, S.-H. (2017). "Conditional random field reliability analysis of a cohesion-frictional slope." *Computers and Geotechnics*, 82, 173-186.

Liu, Y., Lee, F.-H., Quek, S.-T., Chen, E.J., and Yi, J.-T. (2015). "Effect of spatial variation of strength and modulus on the lateral compression response of cement-admixed clay slab." *Géotechnique*, 65(10), 851-865.

Namikawa, T. (2016). "Conditional probabilistic analysis of cement-treated soil column strength." *International Journal of Geomechanics*, 16(1), 04015021.

Namikawa, T., and Koseki, J. (2013). "Effects of spatial correlation on the compression behavior of a cement-treated column." *Journal of Geotechnical and Geoenvironmental Engineering, ASCE*, 139(8), 1346-1359.

Navin, M.P. (2005). *Stability of embankments founded on soft soil improved with deep-mixing-method columns*, Doctoral Thesis, Virginia Polytechnic Institute and State University,Blacksburg, VA, USA.

Navin, M.P., and Filz, G.M. (2006). "Reliability of deep mixing method columns for embankment support." *GeoCongress: Geotechnical Engineering in the Technology Age*.

Tang, Y.X., Miyazaki, Y., and Tsuchida, T. (2001). "Practices of reused dredgings by cement treatment." *Soils and Foundations*, 41(5), 129-143.

U. S. Army Corps of Engineers. (1995). *Introduction to probability and reliability methods for use in geotechnical engineering. Eng. Tech. Letter No 1110-2-547*. U.S. Army Corps of Engineers, CECW-ED.

Yapage, N.N.S., and Liyanapathirana, D.S. (2014). "A parametric study of geosynthetic-reinforced column-supported embankments." *Geosynthetics International*, 21(3), 213-232.

Yapage, N.N.S., Liyanapathirana, D.S., Kelly, R.B., Poulos, H.G., and Leo, C.J. (2014). "Numerical modeling of an embankment over soft ground improved with deep cement mixed columns: Case history." *Journal of Geotechnical and Geoenvironmental Engineering*, 140(11), 04014062.

Zhang, R.-J., Hasan, M.S.M.S., Zheng, J.-J., and Cheng, Y.-S. (2017). "Effect of spatial variability of engineering properties on stability of a CSMC embankment." *Marine Georesources & Geotechnology*.